Hybrid Active Contour Model for Segmentation of Synthetic and Real Images

Ehtesham Iqbal, Asim Niaz, Asad Munir and Kwang Nam Choi

October 3, 2021

HYBRID ACTIVE CONTOUR MODEL FOR SEGMENTATION OF SYNTHETIC AND REAL IMAGES

Ehtesham Iqbal[1], *Asim Niaz*[1], *Asad Munir*[2], *Kwang Nam Choi*[1]

[1]Department of Computer Science and Engineering, Chung-Ang University, Seoul, Republic of Korea.

[2]Dept. of Computer Science, University of Udine Italy

ABSTRACT

Level set models are extensively used for image segmentation because of their capability to handle topological changes. In this paper, the proposed model uses combined local image information and global image information to evolve the contour around the object boundary, making it robust, irrespective of the inhomogeneity. The proposed model is capable to deal with bias conditions, such as intensity inhomogeneity and light effects. We test this model on synthetic, and real images, confirming its superiority over previous models.

***Keywords*—** image segmentation, level set

1. LEVEL SET FORMULATION

Active Contour Models (ACMs) are extensively used for image segmentation. Global-region based ACMs can segment homogeneous regions with assumption that the objects are of homogeneous intensities; however, real images contain inhomogeneity undetected by the such models.

Suppose, we have an image $I(x)$ in R^2. Ω is a bounded open subset of the given domain, with $\partial\Omega$ as its boundary. A parameterized curve is represented by $C(s) : [0, 1] \rightarrow R^2$, dividing image I into two regions, $inside(C)$, and $outside(C)$. C-V [1] function for the homogeneous image segmentation is

$$E_{CV}(C, c_1, c_2) = \lambda_1 \int_\Omega |I(x) - c_1|^2 H_\epsilon(\phi(x))dx + \lambda_2 \int_\Omega |I(x) - c_2|^2 (1 - H)_\epsilon(\phi(x)))dx + \mu \int_\Omega \delta(\phi(x))|\nabla\phi(x)|dx + v \int_\Omega H_\epsilon(\phi(x))dx \quad (1)$$

where λ_1, λ_2, and v are the positive coefficients. c_1, and c_2 are the average intensity means of the inner and outer regions of contour C in image I, defined as

$$c_1 = \frac{\int_\Omega I(x)H_\epsilon\phi(x))dx}{\int_\Omega H_\epsilon(\phi(x)))} \quad (2)$$

$$c_2 = \frac{\int_\Omega I(x)(1 - H_\epsilon\phi(x)))dx}{\int_\Omega(1 - H_\epsilon(\phi(x)))} \quad (3)$$

$$H_\epsilon(\phi(x)) = \frac{1}{2}\left(1 + \frac{2}{\pi} arctan\left(\frac{\phi}{\epsilon}\right)\right) \quad (4)$$

$H_\epsilon(\phi)$ is the smooth approximation of Heaviside function. VLSBC [4] defines an image to be

$$I(x) = b(x)J(x) + n(x), \qquad x \in \Omega \quad (5)$$

where $b(x)$, and $n(x)$ are bias field and noise, respectively. $J(x)$ is the inhomogeneity free, true image, represented as

$$J(x) = \Sigma_{i=1}^{N} l_i M_i(\phi) \quad (6)$$

The local clustering K-means, is the minimization of

$$E \approx \int \left(\Sigma_{i=1} \int_{\Omega i}^{N} K_\sigma(x - y)|I(y) - b(x)c_i|^2 dy\right) dx \quad (7)$$

Using Heaviside function, (7) becomes

$$E = \int \left(\Sigma_{i=1} \int_{\Omega i}^{N} K_\sigma(x - y)|I(y) - b(x)m_i|^2 M_i(\phi)dy\right) dx \quad (8)$$

Here $N = 2$, and M_i accounts for the region member functions i.e $M_1 = H(\phi)$, $M_2 = 1-H(\phi)$. Taking first derivative of (8), we get:

$$b(x) = \Sigma_i^N \frac{K_\sigma * (I(x)m_i M_i(\phi))}{K_\sigma * (c_i^2 M_i(\phi)),} \quad (9)$$

$$m_i = \int \frac{K_\sigma * (I(x)b(x)M_i(\phi))}{K_\sigma * \left(b(x)^2 M_i(\phi)\right)}. \quad (10)$$

We combine local and global fitting energies as

$$E_{Proposed} = \int ((I(x) - I_{bLFI})(I(x) - I_{GFI}))dx \quad (11)$$

where I_{bLFI} and I_{GFI} are the local image fitted and global image fitted models, respectively and are defined as follows:

$$I_{bLFI} = b(x)(m_1 M_1 + m_2 M_2) \quad (12)$$

$$I_{GFI} = c_1 M_1 + c_2 M_2 \quad (13)$$

By calculus of variation [16], (11) minimizes to

$$\frac{\partial\phi}{\partial t} = \delta_\epsilon(\phi)(I(x) - I_{bLFI}(x))(c_1 - c_2) + \delta_\epsilon(\phi)(I(x) - I_{GFI}(x))(m_1 - m_2) \quad (14)$$

where $\delta_\epsilon(\phi)$ is Dirac delta function [1]. Eq (14) is the final equation for evolving the contour. Proposed algorithm is:

MSIT (Ministry of Science and ICT) Korea supports this research, under the National Program for Excellence in SW(20210100) supervised by the Institute of Information and communications Technology Planning and Evaluation in 2021. Corresponding Author: Kwang Nam Choi: knchoi@cau.ac.kr

Algorithm 1 Proposed Algorithm

Input Image $I(x)$ with $b(x) = 0$.

1) Initialize levelset ϕ from $p = 0$,

$$\phi_{x,t=0} = \begin{cases} -p, & x \in \Omega_0 - \partial\Omega_0 \\ 0, & x \in \partial\Omega_0 \\ p, & x \in \Omega - \partial\Omega_0 \end{cases}$$

2) $Iteration\ count from$ n=0.

3) $Compute$ m_i using (10) and c_i by using (2) and (3).

4) Solve PDE (14) in ϕ to obtain $\phi_{(t+1)}$.

5) Regularize the function by a Gaussian filter.

6) If solution converges, stop. If not, $n = n + 1$.

7) Output: Final image segmentation is obtained.

2. EXPERIMENTAL RESULTS

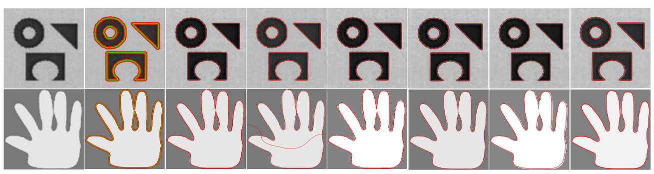

Fig. 1. Synthetic images: (col 1) input image, (col 2) C-V [1], (col 3) LBF [2], (col 4) LIF [3], (col 5) VLSBC [4], (col 6) Zhang et. al [5], (col 7) FRAGL [6] (col 8), Proposed model.

This section presents results of the proposed method along-with previous methods. Fig. 1 and Fig. 2 shows results of different ACMs over synthetic and real example images, respectively. For Fig. 1, C-V [1] in Row 2 produced smooth contour around the fingers boundaries, but it failed to separate middle finger, because of absence of local statistics. Utilizing local image fitting energy, the LIF [3] distinguished middle fingers boundaries, but false contour appearance limits accuracy. LBF [2], and VLSBC [4] produce similar results, while the accuracy of Zhang et al. [5] model is comparatively less than all. Real images are taken from medical images, dermoscopic images of PH2 database [7], and skin lesion images of skin-cancer-mnist-ham10000 database [8] in Row 1, 2, and 3, respectively. Fig. 2 shows that the FRAGL [6] method produces results almost same as the proposed method. C-V [1] model fails to dealt wih inhomogeneity in images, producing noisy segmentation. LBF [2], and LIF [3] models captured the ROI, but false contour appearances compromise accuracy. Table I presents Accuracy metric values of all the in-comparison methods, confirming efficiency of our method.

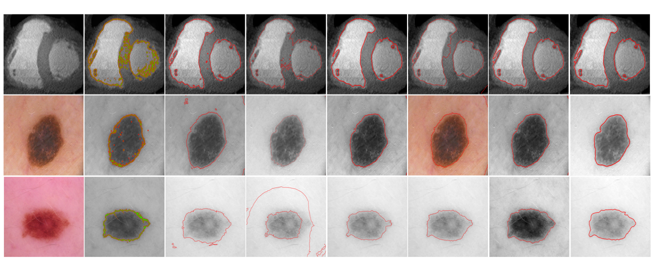

Fig. 2. Real images: (col 1) input image, (col 2) C-V [1], (col 3) LBF [2], (col 4) LIF [3], (col 5) VLSBC [4], (col 6) Zhang et. al [5], (col 7) FRAGL [6], (col 8) Proposed model.

Table 1. Segmentation Accuracy Metric

Method	[1]	[8]	[9]	[10]	[11]	[12]	Our
Accuracy	0.71	0.85	0.87	0.91	0.92	0.95	0.98

3. CONCLUSION

In this paper, a novel method for inhomogeneous image segmentation, combining local and global fitting models, smoothed by Gaussian filtering , is presented. Our model efficiently dealt with the bias conditions outclassing other segmentation methods. Experimental results confirm the superiority of the proposed model.

4. REFERENCES

[1] T. Chan et al., "Active contours without edges," IEEE Trans. Image. Process., vol. 10, no. 2, , 2 (2001), pp. 266–277

[2] C.M. Li et al., "Implicit active contours driven by local binary fitting energy", in: Proceeding of CVPR2007, 07', pp. 1-7.

[3] C.M. Li et al., "Implicit active contours driven by local binary fitting energy", in: Proceeding of CVPR2007, 07', pp. 1-7.

[4] C. Li et al., "A Level Set Method for Image Segmentation in the Presence of Intensity Inhomogeneities With Application to MRI," in IEEE Trans. Image. Process., vol. 20, no. 7, 7 (2011), pp. 2007-2016

[5] K. Zhang et al., "A Level Set Approach to Image Segmentation With Intensity Inhomogeneity," in IEEE Trans. Cybernetics, vol. 46, no. 2, 2 (2016), pp. 546-557

[6] J. Fang et al., "Fuzzy region-based active contours driven by weighting global and local fitting energy," IEEE Access, 12 (2019).

[7] T. Mendonca et al.. PH^2 - A dermoscopic image database for research and benchmarking, 35th International Conference of the IEEE Engineering in Medicine and Biology Society, 7 (2013), Osaka, Japan.

[8] P. Tschandl. 2018. Harvard Dataverse. https://doi.org/10.7910/DVN/DBW86T